Alternatively spliced proline-rich cassettes link WNK1 to aldosterone action

Ankita Roy,[1] Lama Al-Qusairi,[2] Bridget F. Donnelly,[1] Caroline Ronzaud,[2] Allison L. Marciszyn,[1] Fan Gong,[1] Y.P. Christy Chang,[3] Michael B. Butterworth,[4] Núria M. Pastor-Soler,[1,4] Kenneth R. Hallows,[1,4] Olivier Staub,[2] and Arohan R. Subramanya[1,4,5]

[1]Department of Medicine, University of Pittsburgh School of Medicine, Pittsburgh, Pennsylvania, USA. [2]Department of Pharmacology and Toxicology, University of Lausanne, Lausanne, Switzerland. [3]Department of Medicine, University of Maryland Medical School, Baltimore, Maryland, USA. [4]Department of Cell Biology, University of Pittsburgh School of Medicine, Pittsburgh, Pennsylvania, USA. [5]VA Pittsburgh Healthcare System, Pittsburgh, Pennsylvania, USA.

The thiazide-sensitive NaCl cotransporter (NCC) is important for renal salt handling and blood-pressure homeostasis. The canonical NCC-activating pathway consists of With-No-Lysine (WNK) kinases and their downstream effector kinases SPAK and OSR1, which phosphorylate NCC directly. The upstream mechanisms that connect physiological stimuli to this system remain obscure. Here, we have shown that aldosterone activates SPAK/OSR1 via WNK1. We identified 2 alternatively spliced exons embedded within a proline-rich region of WNK1 that contain PY motifs, which bind the E3 ubiquitin ligase NEDD4-2. PY motif–containing WNK1 isoforms were expressed in human kidney, and these isoforms were efficiently degraded by the ubiquitin proteasome system, an effect reversed by the aldosterone-induced kinase SGK1. In gene-edited cells, WNK1 deficiency negated regulatory effects of NEDD4-2 and SGK1 on NCC, suggesting that WNK1 mediates aldosterone-dependent activity of the WNK/SPAK/OSR1 pathway. Aldosterone infusion increased proline-rich WNK1 isoform abundance in WT mice but did not alter WNK1 abundance in hypertensive *Nedd4-2* KO mice, which exhibit high baseline WNK1 and SPAK/OSR1 activity toward NCC. Conversely, hypotensive *Sgk1* KO mice exhibited low WNK1 expression and activity. Together, our findings indicate that the proline-rich exons are modular cassettes that convert WNK1 into a NEDD4-2 substrate, thereby linking aldosterone and other NEDD4-2–suppressing antinatriuretic hormones to NCC phosphorylation status.

Introduction

With-No-Lysine (WNK) kinases are large serine-threonine kinases that regulate sodium, potassium, and blood-pressure homeostasis. WNKs participate in these processes by coordinating multiple electrolyte transport pathways in more distal segments of the nephron (reviewed in ref. 1). Mutations in *WNK1*, *WNK4*, and the KLHL3/CUL3 complex, which regulates WNK abundance, are 4 known genes that cause familial hyperkalemic hypertension (FHHt, PHA2, Gordon Syndrome), a Mendelian disorder of thiazide-sensitive hypertension, hyperkalemia, and normal glomerular filtration rate (2). WNK1 and WNK4 are key regulators of renal sodium–coupled cation chloride cotransporters, including the thiazide-sensitive NaCl cotransporter (NCC) of the distal convoluted tubule (DCT) and the $Na^+/K^+/2Cl^-$ cotransporter (NKCC2) of the thick ascending limb (TAL). Both WNKs stimulate NCC and NKCC2 indirectly by activating 2 downstream and structurally homologous serine-threonine kinases, the Ste20- and SPS1-related proline alanine-rich kinase (SPAK) and oxidative stress responsive kinase 1 (OSR1). WNK1 and WNK4 activate SPAK/OSR1 by phosphorylating residues in their kinase domains and C-termini (3). Once activated, SPAK and OSR1 directly phosphorylate the intracellular amino termini of NCC and NKCC2, increasing their transport activity (4).

Several hormones that regulate renal tubular salt reabsorption and blood pressure — including aldosterone, angiotensin II, insulin, and vasopressin — activate NCC and/or NKCC2 (5–8). Although each of these hormones act via their own sets of receptors and signaling pathways, they all trigger downstream SPAK/OSR1 phosphorylation as a precursor to cation-chloride cotransporter activation. Thus, the diverse signal transduction networks utilized by these hormones likely converge upon WNK kinases to enhance NaCl cotransport. Current evidence indicates that hormones that stimulate renal NaCl reabsorption recruit specific WNK kinases to mediate their effects (5). However, due to deficiencies in our understanding of WNK kinase structure and domain organization, the molecular mechanisms that allow these hormones to interact with WNKs and trigger SPAK/OSR1 activation remain obscure.

In this study, we identify a molecular mechanism that explains how aldosterone can interface with the WNK signaling pathway to influence SPAK/OSR1 activity and downstream NCC activation. We show that WNK1 is an aldosterone-induced protein that contains functional "PY motifs," which are short-linear proline-containing sequences that bind to an E3 ubiquitin ligase critical for the aldosterone response, NEDD4-2. NEDD4-2 accelerates the rate of WNK1 turnover, and this process is attenuated by the serum- and glucocorticoid-regulated kinase 1 (SGK1), the canonical kinase that transduces aldosterone-dependent signals downstream of the mineralocorticoid receptor (MR) (9). Notably, the PY motifs are exclusively contained within 2 adjacent proline-rich exons that undergo tissue-specific alternative splicing. This suggests that the NEDD4-2 interaction surface resides within modular cassettes that can be added to or removed from the WNK1 sequence, depending on physiological need. Thus, we suggest that inclusion
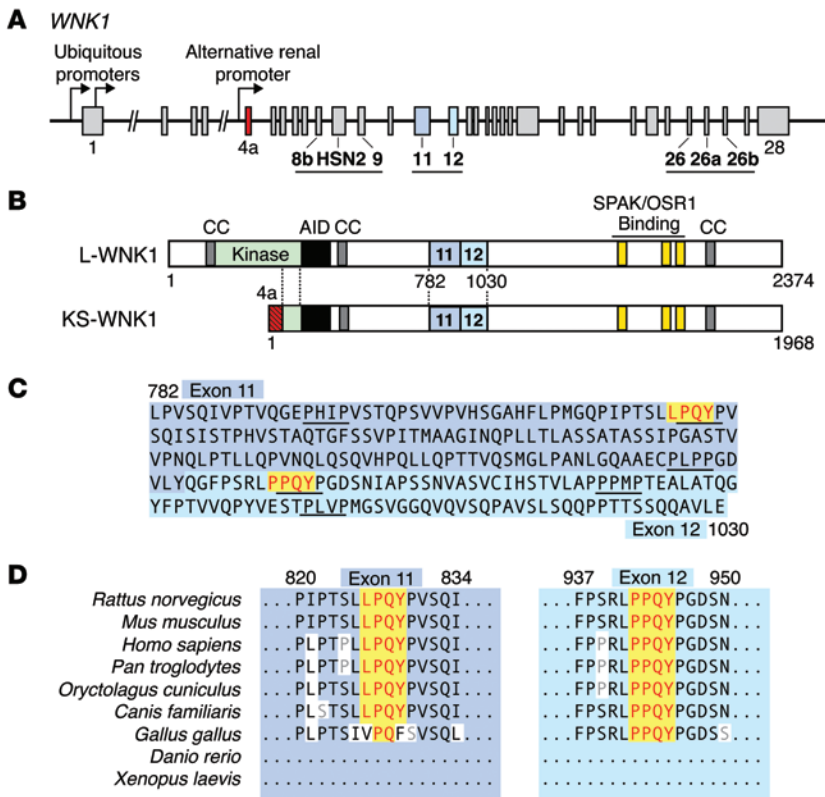
Figure 1. Identification of 2 PY motifs in exons 11 and 12 of *WNK1*. (**A**) Schematic representation of the *WNK1* gene. Two ubiquitous promoters drive the transcription of *WNK1* isoforms containing an intact kinase domain (L-WNK1). A renal promoter drives the expression of a kidney-specific transcript (KS-WNK1). Regions of *WNK1* that undergo tissue-specific alternative splicing are underlined. Exon 4a, which encodes a short N-terminal sequence unique to KS-WNK1, is shown in red. Exons 11 and 12 are highlighted in blue. (**B**) Domain structure of L-WNK and KS-WNK1. The location of 3 coiled coil domains (CC) that facilitate WNK complex formation (65), an autoinhibitory domain (AID) that suppresses WNK kinase activity (66), and C-terminal SPAK/OSR1 binding motifs are shown. Downstream of exon 4a, L-WNK1 and KS-WNK1 are identical. (**C**) Amino acid sequence of rat exons 11 and 12. Two canonical PY motifs are highlighted in yellow. The exons are proline rich and contain numerous PXXP motifs. (**D**) The PY motifs in exons 11 and 12 are highly conserved in mammals. The exons are not present in nonmammalian organisms, such as *Xenopus*, zebrafish, *Drosophila*, and *C. elegans*.

of these exons into the WNK1 coding sequence converts WNK1 into a NEDD4-2 substrate that allows aldosterone and potentially other hormones to modulate the activity of SPAK, OSR1, and their downstream targets.

Results

WNK1 gene structure and identification of putative NEDD4-2 interaction sites in exons 11 and 12. *WNK1* is a large, 32-exon gene spanning approximately 160 kilobases in humans. Three regions downstream of the kinase domain undergo alternative splicing (Figure 1A; ref. 10). Additionally, *WNK1* contains multiple promoters that generate 2 functionally distinct classes of isoforms. Two proximal promoters drive the expression of ubiquitously expressed long isoforms (L-WNK1) that contain a full kinase domain and therefore are capable of phosphorylating downstream targets (11). A third promoter located in intron 4 generates truncated isoforms that lack kinase activity and are exclusively expressed in the kidney (Figure 1B). These kidney-specific isoforms (KS-WNK1) are expressed in the DCT and connecting tubule (CNT), and to a lesser extent in the TAL and cortical collecting duct (CCD) (10). The renal promoter that drives KS-WNK1 expression replaces the first 4 exons of *WNK1* with a kidney-specific exon termed exon 4a; downstream from this short and unique sequence, the primary structures of L-WNK1 and KS-WNK1 are identical.

All WNK family members contain proline-rich regions located at the amino terminus and in the middle of their polypeptide sequences. We reasoned that PY motifs might be present in these areas. PY motifs bind to proteins that contain WW domains (12) and have been reported to participate in aldosterone-dependent signaling cascades. For example, each of the 3 epithelial sodium

channel (ENaC) subunits contain these sequences embedded within their C-terminal cytoplasmic domains, which interact with WW domains of the E3 ligase NEDD4-2 (13). In the presence of aldosterone, distal nephron MRs stimulate SGK1 transcription and protein activation. This serine-threonine kinase phosphorylates specific residues on NEDD4-2 that reduce interaction with ENaC, diminishing ENaC ubiquitylation and degradation (14).

Given their role in aldosterone signaling, we screened WNK kinases for classical PY motifs, corresponding to the sequence [L/P]PXY (15). These signatures were identified in 2 WNK family members, WNK1 and WNK2 (Figure 1C and data not shown). In both cases, the motifs were positioned within proline-rich regions located in the mid-portion of the protein. Since WNK2 is not expressed in the kidney (16), we focused our attention on WNK1 as a potential posttranslational target for aldosterone action. The 2 PY motifs in WNK1 reside within exons 11 and 12, both of which undergo alternative splicing (11, 17). As shown in Figure 1D, the 2 motifs are highly conserved among terrestrial mammals but are absent in amphibians and freshwater fish, suggesting that they may play an evolutionary role in fine-tuning the conservation of electrolytes and water.

WNK1 isoforms containing PY motifs are expressed in the aldosterone-sensitive distal nephron. Since previous studies in rodents indicated that exons 11 and 12 of *WNK1* undergo alternative splicing in multiple tissues, we sought to confirm that these PY motif–containing exons are expressed in the human kidney. To this end, reverse transcription PCR studies (RT-PCR studies) were performed on adult human kidney mRNA. These studies confirmed that the region spanning exons 11–12 is extensively spliced in kidney (Supplemental Figure 1; supplemental material available online with
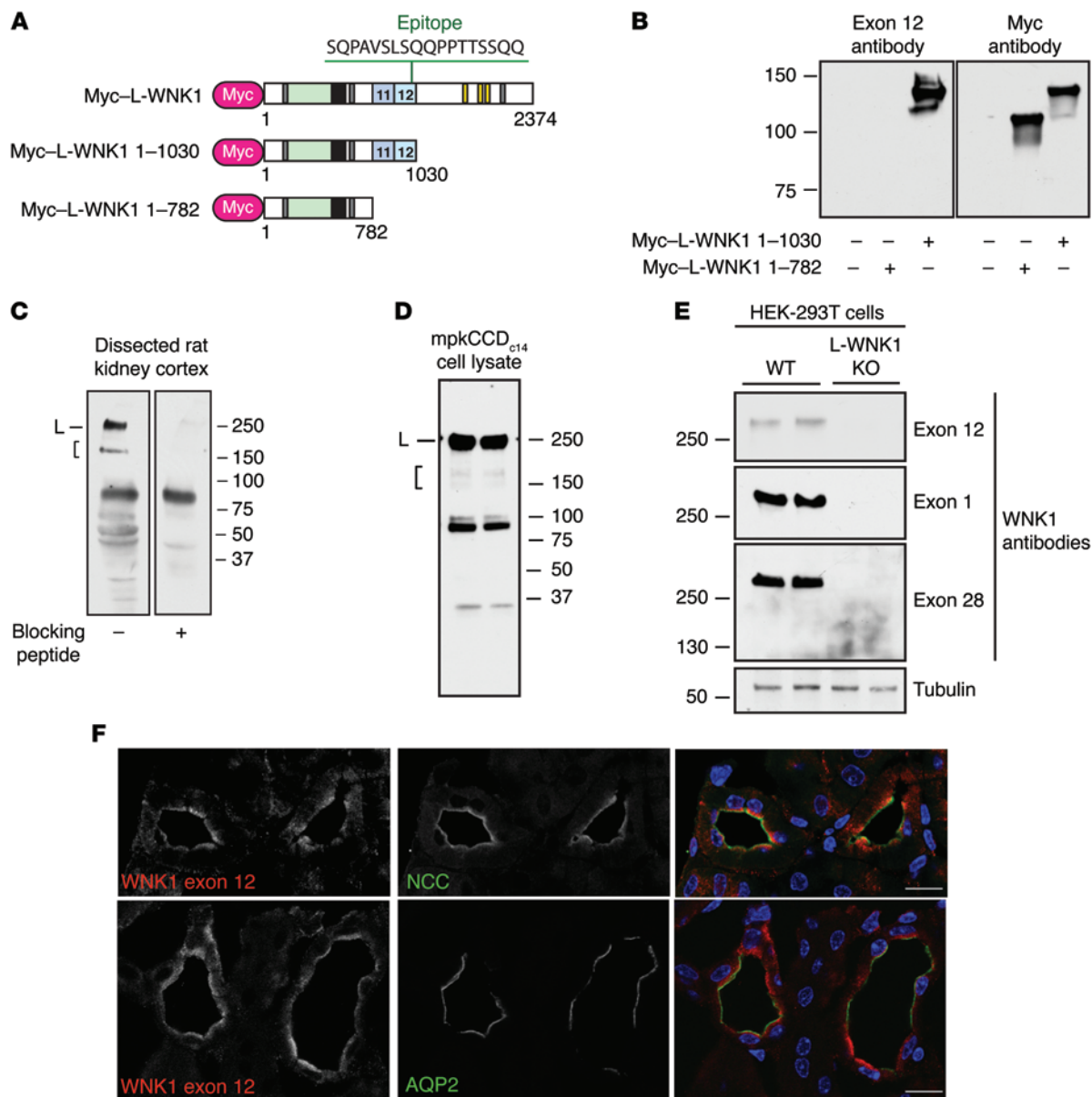
Figure 2. WNK1 isoforms containing PY motifs are expressed in the ASDN. (**A**) Schematic representation of N-terminally Myc-tagged cDNAs used for exon 12 antibody validation. Rabbit antisera to WNK1 were generated to the indicated exon 12 epitope. (**B**) The exon 12 antibody specifically recognizes a Myc-tagged L-WNK1 fragment containing exon 12 that was transiently expressed in HEK-293T cells. (**C**) Immunoblots of dissected rat kidney cortex homogenates (50 μg) probed with the exon 12 antibody revealed a discrete band at approximately 250 kDa, corresponding to the MW of L-WNK1 (L), and shorter species migrating between 150 and 250 kDa, consistent with KS-WNK1 and/or C-terminal proteolytic fragments of L-WNK1 (bracket). Both high-MW bands were not seen when the antibody was preincubated with excess immunizing peptide. Several lower-MW species were also quenched with peptide competition. A nonspecific band was noted between 75 and 100 kDa. (**D**) Bands of similar MWs were noted in mpkCCD$_{c14}$ CCD cells. (**E**) Along with 2 other WNK1-specific antibodies, the antisera recognized a band at approximately 250 kDa in HEK-293T cells that was absent in genetically validated L-WNK1 KO cells (19). (**F**) Immunostaining of mouse kidney with exon 12 antisera revealed a tubule-specific signal that colocalized with NCC in DCT and aquaporin-2 (AQP2) in CCD. Scale bars: 10 μm. See also Supplemental Figures 1 and 2.

this article; doi:10.1172/JCI75245DS1). Additional RT-PCR amplifications verified that these splicing events occur in both L- and KS-WNK1 (Supplemental Figure 2). Collectively, these data confirm that kinase-active and -deficient isoforms of WNK1 expressed in the human kidney contain a complete assortment of exon 11 and 12 combinations. These findings are consistent with prior work by O'Reilly et al. (17) and Delaloy et al. (11), as well as an analysis of *WNK1* transcripts that was performed by Vidal-Petiot et al. in 2012

(10). Notably, this more recent study also found that exon 12 is highly represented in kidney relative to other tissues and is enriched in the aldosterone-sensitive distal nephron (ASDN), suggesting that it plays an important role in renal salt transport physiology.

To determine whether WNK1 proteins containing PY motifs are expressed in the distal nephron, we generated affinity-purified antisera to a peptide epitope located within exon 12 of WNK1 (Figure 2A). The antisera specifically recognized a recombinant Myc
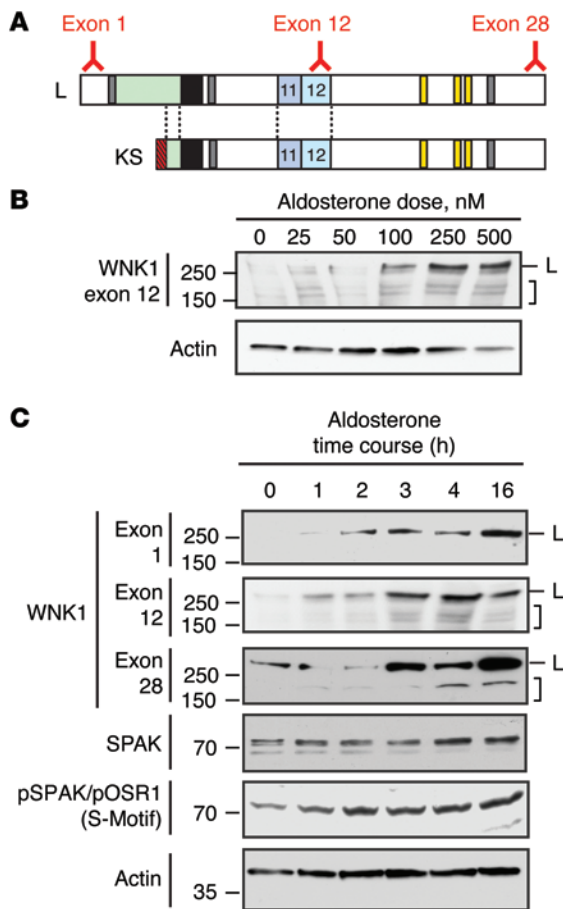
Figure 3. WNK1 is an aldosterone-induced protein. (**A**) Location of epitopes for the 3 exon-specific anti-WNK1 antibodies used in the immunoblots below. The exon 1 antibody selectively recognizes L-WNK1, while the exon 12 and 28 antibodies detect both L- and KS-WNK1. (**B**) Nanomolar doses of aldosterone increased total WNK1 protein abundance in mpkCCD$_{c14}$ cells over 4 hours. High-MW signals at approximatley 250 kDa, corresponding to L-WNK1 (L) and lower-MW species corresponding to KS-WNK1 and/or proteolytic fragments of L-WNK1 (bracket) are noted. (**C**) 100 nM aldosterone increased total WNK1 protein abundance over a 16-hour timecourse in mpkCCD$_{c14}$ cells. (**D**) Total SPAK and phosphorylated SPAK/OSR1 abundance were also increased in the presence of aldosterone. The "S-motif" antibody detects regulatory domain phosphorylation at Ser373 of SPAK and Ser325 of OSR1, a marker of SPAK/OSR1 activation (3). $n = 4$; *$P < 0.05$ for both total SPAK and pSPAK/OSR1 by 1-Way ANOVA Dunnett's post hoc comparison to the abundance at time zero. See also Supplemental Figure 3.

epitope–tagged L-WNK1 fragment containing exon 12 that was transiently transfected into HEK-293T cells (Figure 2B); in dissected rat kidney cortex, the antibody recognized high-MW signals that were quenched when the antiserum was incubated with excess immunizing peptide (Figure 2C). This was observed for a major band at 250 kDa, corresponding to the MW of L-WNK1, and for shorter species that migrated between 150 and 250 kDa, corresponding to KS-WNK1 and/or C-terminal proteolytic fragments of L-WNK1. The exon 12 antisera also recognized bands of similar MW in mpkCCD$_{c14}$ cells, an aldosterone-sensitive epithelial model of the CCD (Figure 2D; ref. 18). The major L-WNK1–specific band at approximately 250 kDa was also detected in WT HEK-293T cells but not in previously validated L-WNK1 KO HEK-293T cells that were generated by CRISPR/Cas-mediated gene editing (Figure 2E; ref. 19). In immunofluorescence confocal microscopy, antisera directed against the exon 12 epitope detected a tubule-specific signal in aldosterone-sensitive tissues that colocalized near plasma membranes with NCC in the DCT, and in cells of the CCD, marked by aquaporin-2 costaining (Figure 2F).

WNK1 is an aldosterone-induced protein. The observation that WNK1 isoforms containing canonical PY motifs are expressed in the ASDN suggests that they may be aldosterone-regulated. To begin to evaluate this, we sought to measure WNK1 expression in response to aldosterone in a cell-culture model of the distal nephron. We initially screened mDCT cells for these studies, as these cells are commonly used to study DCT physiology. However, we were unable to detect KS-WNK1 expression in this cell line. We

were, however, able to detect both L- and KS-WNK1 at the transcript level in mpkCCD$_{c14}$ cells. Thus, we decided to perform our initial analysis of the effects of aldosterone on WNK1 function in this model. In mpkCCD$_{c14}$ cells, dose-response tests indicated that the abundance of WNK1 isoforms increased as the concentration of aldosterone was titrated from 0–500 nM (Figure 3A). This was observed for high-MW species corresponding to long and short forms of WNK1. In addition, treatment with 100 nM aldosterone increased WNK1 abundance over a 16-hour timecourse (Figure 3B). This effect was seen with 3 antibodies targeting different WNK1 epitopes, including an N-terminal L-WNK1–specific antibody to exon 1 and two C-terminal antibodies directed to exons 12 and 28. Aldosterone also increased total SPAK abundance and SPAK/OSR1 phosphorylation, detected with an antibody that recognizes known WNK1 regulatory S-motif phosphosites at serine 383 of SPAK and serine 325 of OSR1 (3) (Figure 3, C and D).

A previous report found that a noncoding RNA, miR-192, negatively regulated *WNK1* mRNA abundance and was suppressed by aldosterone (20). We therefore reasoned that aldosterone-induced downregulation of miR-192 might explain the increase in WNK1 expression observed in mpkCCD$_{c14}$ cells. However, 100 nM aldosterone did not reduce miR-192 expression in these cells over a 16-hour timecourse, as measured by quantitative PCR (qPCR) (Supplemental Figure 3, A and B). Consistent with this observation, 100 nM aldosterone did not trigger an increase in the abundance of mRNA encoding KS-WNK1, L-WNK1, or exon 12–containing WNK1 isoforms in mpkCCD$_{c14}$ cells over a timecourse of
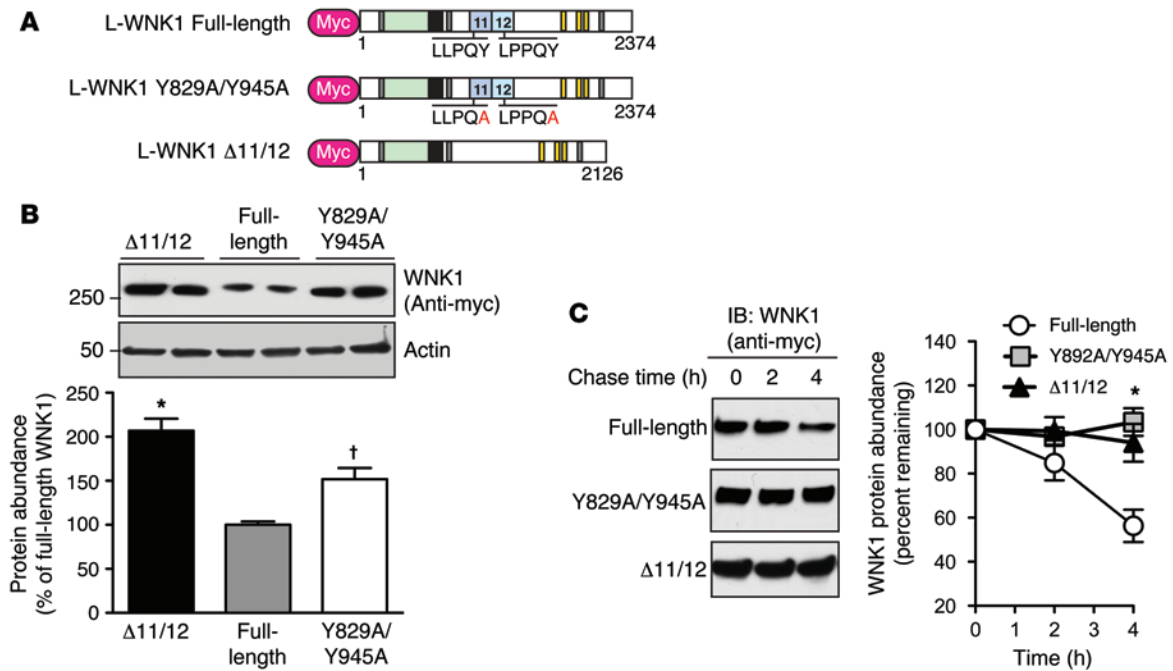
Figure 4. Exons 11 and 12 destabilize WNK1 in a PY motif–dependent manner. (**A**) Schematic comparing Myc-tagged WT full-length L-WNK1, PY motif–null L-WNK1 (Y829A/Y945A), and a previously reported natural L-WNK1 splice variant lacking exons 11 and 12 (Δ11/12). (**B**) Steady-state abundance of full-length L-WNK1 was less than the PY-null mutant or L-WNK1 Δ11/12. $n = 6$; $*P < 0.001$ or $^{\dagger}P < 0.01$ by 1-way ANOVA, Dunnett's post hoc comparison to full-length L-WNK1. (**C**) Stability of Myc-tagged L-*WNK1* cDNAs in HEK-293T cells. Cells transiently expressing full-length L-WNK1, PY motif–null L-WNK1, or the Δ11/12 splice variant were treated with CHX (100 μg/ml) 24 hours after transfection and chased for 4 hours. Right panel, plot of L-WNK1 abundance during the time course, expressed as a percentage of the starting material at time zero. $n = 4$; $*P < 0.05$ by 1-way ANOVA, Dunnett's post hoc comparison of either the PY motif–null mutant or the Δ11/12 splice variant to full-length L-WNK1 at the 4-hour time point.

24 hours (Supplemental Figure 3, C and D). The same mpkCCD$_{c14}$ cells, however, did exhibit a transcriptional response to 100 nM aldosterone, as we were able to detect a progressive increase in *Sgk1* mRNA abundance (Supplemental Figure 3D). Although these data do not match previous reports indicating that aldosterone induces the transcription of KS-WNK1 both in MR-transfected M1 cells and in vivo (21, 22), the data do indicate that the stimulatory effect of 100 nM aldosterone on WNK1 protein expression observed in mpkCCD$_{c14}$ cells is not due to an effect on *Wnk1* mRNA transcription, implicating posttranslational mechanisms as an alternative explanation.

Exons 11 and 12 destabilize L-WNK1 in a PY motif–dependent manner. To determine whether the 2 PY motifs in exons 11 and 12 of WNK1 are functional, we assessed the steady-state protein abundance of epitope-tagged L-WNK1 constructs following transient expression in HEK-293T cells, a cell line that endogenously expresses NEDD4-2 and its closely related isoform NEDD4-1 (23). The total protein abundance of Myc-tagged L-WNK1 was compared with L-WNK1 Δ11/12, a previously described PY motif–deficient L-WNK1 splice variant (24), and L-WNK1 Y829A/Y945A, a PY-null mutant lacking the tyrosines that are critical for WW domain interaction (Figure 4A; ref. 25). As shown in Figure 4B, the steady-state abundance of the Δ11/12 variant and the PY-null mutant were both significantly increased relative to full-length L-WNK1. To determine if these differences were due to altered protein stability, we performed a cycloheximide (CHX) chase assay to monitor the timecourse of protein degradation after arresting translation. In these studies, the Δ11/12 and PY-null

L-WNK1 constructs were more resistant to protein degradation than the WT full-length protein (Figure 4C), suggesting that the PY motifs in exons 11 and 12 decrease WNK1 stability, possibly via interaction with NEDD4-2.

Nedd4-2 targets PY motif–containing WNK1 isoforms for degradation via the ubiquitin proteasome system. To test whether endogenously expressed NEDD4 E3 ligases regulate WNK1 abundance in HEK-293T cells, we conducted an RNA interference (RNAi) study. Transfection of pan-NEDD4 siRNAs targeting human NEDD4-1 and NEDD4-2 increased the steady-state protein expression of endogenous L-WNK1 isoforms containing exon 12, relative to cells transfected with a scrambled siRNA control (Figure 5A). WNK4 protein expression was unaltered, indicating that the effect was specific for WNK1. In overexpression experiments, WT NEDD4-2 consistently decreased steady-state full-length L-WNK1 abundance at 3 different transfection ratios (Figure 5B); in contrast, a dominant-negative NEDD4-2 mutant lacking catalytic activity had no effect (NEDD4-2 C938S; ref. 26). Consistent with these findings, overexpressed WT NEDD4-2 accelerated L-WNK1 degradation in CHX chase assays, an effect that was attenuated when the WT E3 ligase was substituted with the dominant-negative NEDD4-2 mutant, or when WT NEDD4-2 was coexpressed with PY-null mutant L-WNK1 (Figure 5C). In HEK-293T cells, NEDD4 isoforms coimmunoprecipitated with overexpressed WT L-WNK1 and exhibited decreased interaction with the PY-null mutant and the Δ11/12 L-WNK1 isoform (Figure 5D). Moreover, in mpkCCD$_{c14}$ epithelia, both long and short forms of WNK1 coimmunoprecipitated in native complexes with NEDD4 isoforms (Figure 5E).
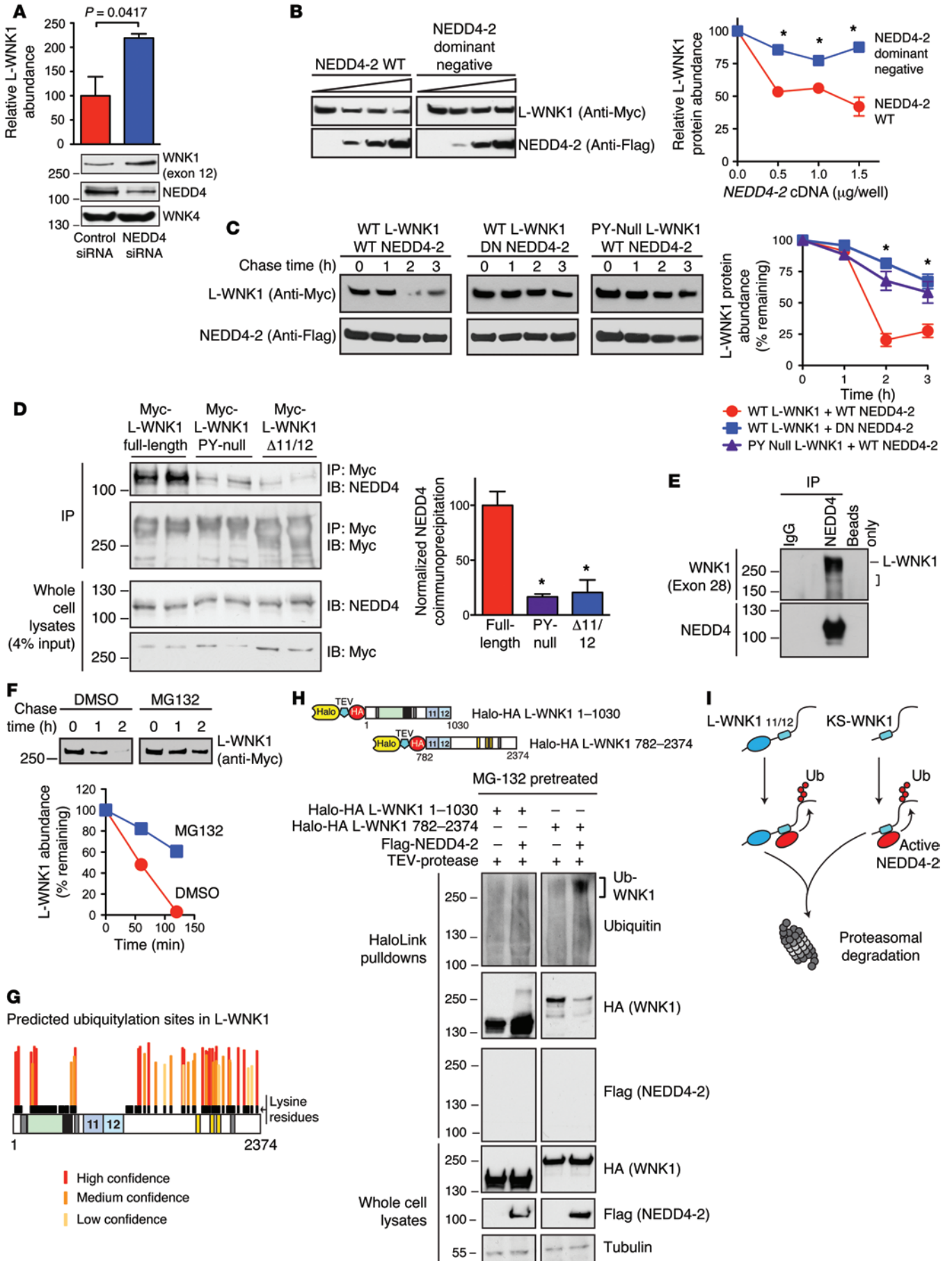
Figure 5. PY motif–containing WNK1 isoforms are NEDD4-2 substrates.
(**A**) Pan-NEDD4 knockdown increases WNK1 abundance in HEK-293T cells. $n = 5$; $P = 0.0417$ by Student's t test. (**B**) WT NEDD4-2 (0–1.5 μg/well) decreased L-WNK1 abundance (0.5 μg/well) in HEK-239T cells; dominant-negative NEDD4-2 (DN; C938S) had no effect. $n = 4$; *$P < 0.01$ by Student's t test for the indicated NEDD4-2 dosages. (**C**) CHX chases in HEK-293T cells. WT NEDD4-2 destabilized WT Myc-L-WNK1 to a greater degree than DN Nedd4-2. PY motif–null L-WNK1 was resistant to WT NEDD4-2. $n = 4$; *$P < 0.01$, by 1-way ANOVA, Dunnett's test. (**D**) Coimmunoprecipitation assay. Left: Anti-Myc immunoprecipitates (IP) from HEK-293T cells transiently expressing Myc-tagged L-WNK1 constructs were immunoblotted (IB) for endogenous NEDD4 isoforms. Right: Quantification of IP results. $n = 4$; *$P < 0.001$, by 1-way ANOVA, Dunnett's test. (**E**) Endogenous co-IP of WNK1 with NEDD4 isoforms in mpkCCD$_{c14}$ cells. L-WNK1 and lower MW species (bracket) were detected. Representative of 3 experiments. (**F**) MG-132 (10 μM) attenuates NEDD4-2 mediated L-WNK1 degradation by CHX chase in HEK-293T cells. Representative of 3 experiments. (**G**) Putative ubiquitylation sites on L-WNK1, stratified by UbPred. Lysine residues are shown in black. Notably, exons 11 and 12 are completely lysine deficient. (**H**) In vivo ubiquitylation assay. Top: N- and C-terminal Halo-HA double-tagged L-*WNK1* cDNAs with TEV cleavage spacer. Bottom: Lysates of MG-132–pretreated HEK293T cells expressing WNK1 fragments +/– Flag–NEDD4-2 were incubated with HaloLink resin. Following covalent pulldown, fragments were washed with SDS to remove autoubiquitylated NEDD4-2 (67), cleaved with TEV, and subjected to immunoblotting. Representative of 4 experiments. (**I**) NEDD4-2 ubiquitylates the WNK1 C-terminus common to both L- and KS-WNK1, marking both species for degradation. See also Supplemental Figures 4 and 5.

Since intact catalytic activity is required for NEDD4-2 to downregulate WNK1 abundance, we asked whether NEDD4-2 targets WNK1 for degradation via the ubiquitin proteasome pathway. Accordingly, we conducted CHX chases in which L-WNK1 was coexpressed with WT NEDD4-2 in the absence and presence of the proteasomal inhibitor MG-132. As shown in Figure 5F, a 4-hour preincubation of HEK-293T cells with 10 μM MG-132 attenuated the rate of L-WNK1 degradation relative to vehicle-treated controls. In silico analysis using the UbPred algorithm (27) identified numerous potential ubiquitylation acceptor lysines on L-WNK1, both at the N- and C-terminal regions of the protein. Most of these were clustered downstream of exon 12 (Figure 5G). Consistent with this prediction, in vivo ubiquitylation assays detected an appropriately sized high-MW smear in HEK-293T cells expressing a PY motif–containing WNK1 C-terminal fragment, and NEDD4-2 coexpression enhanced this signal (Figure 5H). In contrast, no appreciable change above background was observed in NEDD4-2 transfected cells coexpressing the L-WNK1 N-terminus, suggesting that this region was relatively spared from NEDD4-2 ubiquitylation. Ubiquitylation of the WNK1 C-terminus was dependent on intact NEDD4-2 catalytic activity, as no significant ubiquitylation was apparent when the Halo-tagged C-terminus was coexpressed with dominant-negative NEDD4-2 (Supplemental Figure 4A). In addition, C-terminal fragments lacking exons 11 and 12 or containing mutations within the exon 11/12 PY motifs were ubiquitylated less strongly compared with an intact WT C-terminus (Supplemental Figure 4B). Since this C-terminal WNK1 fragment is present in both L-WNK1 and KS-WNK1, these findings indicate that NEDD4-2 targets both isoforms for degradation (Figure 5I).

The *WNK1* cDNAs used for these studies were constructed from the original L-WNK1 clone isolated from brain (AAF74258.1; ref. 24). This clone contains a variant serine located 7 amino acids from the C-terminal end of the protein that replaces a phylogenetically conserved glycine residue (glycine 2368, based on the amino acid numeration for RefSeq XP_008761429.1: the rat L-WNK1 isoform containing exons 9, 11, and 12 studied here). Changing this serine residue back to the conserved glycine enhances its activity toward NCC via SPAK/OSR1 (28). Since serine residues may function as noncanonical sites for ubiquitylation (29), we sought to determine whether this glycine-to-serine variant influences WNK1 stability and NEDD4-2 sensitivity. In CHX chase assays, however, we found that the evolutionarily conserved protein degraded robustly in the presence of NEDD4-2 (Supplemental Figure 5). Degradation of the glycine-amended construct was also dependent on the PY motifs in exons 11 and 12, since inactivating these signatures stabilized the protein significantly (Supplemental Figure 5).

SGK1 inhibits NEDD4-2-mediated downregulation of WNK1. Aldosterone induces the transcription of SGK1, which interferes with NEDD4-2 function by phosphorylating residues that alter PY motif binding, including a canonical "major" site at mouse serine 328 (analogous to *Xenopus* serine 444) (30). To test whether SGK1 can inhibit NEDD4-2–mediated regulation of WNK1, we first tested the effect of small-molecule SGK1 inhibitors on WNK1 abundance in mpkCCD$_{c14}$ cells. Pretreatment with the competitive SGK1 inhibitor GSK650394 or the SGK1 activation blocker LY294002 prevented NEDD4-2 major-site phosphorylation and WNK1 induction (Figure 6A). This indicates that aldosterone is incapable of upregulating WNK1 abundance in the absence of SGK1 activity. Consistent with these findings, coimmunoprecipitation studies in mpkCCD$_{c14}$ cells revealed that the interaction between NEDD4 isoforms and WNK1 was reduced when cells were treated with 100 nM aldosterone (Figure 6B). In CHX chase studies, the rate of L-WNK1 degradation was attenuated when NEDD4-2 was coexpressed with SGK1-S422D, a constitutively kinase-active form of SGK1 (31), when compared with cells transfected with the kinase-dead SGK1 mutant K127M (Figure 6C). Furthermore, coimmunoprecipitation studies with L-WNK1 1-1030, a stable N-terminal L-WNK1 fragment that contains NEDD4-2 binding sites but lacks the C-terminal ubiquitylation hub (Figure 5I), revealed that NEDD4-2 associated more strongly with WNK1 when it was coexpressed with kinase-dead SGK1, rather than the constitutively active S422D form (Figure 6D).

The aforementioned major SGK1 phosphorylation site on NEDD4-2, located at mouse serine 328 (*Xenopus* serine 444), is also accompanied by other "minor" SGK1 phosphorylation sites at mouse serine 222 and threonine 247 (corresponding to *Xenopus* serine 338 and threonine 363) (32). These minor sites are believed to be more SGK1 specific (32). All 3 of these phosphorylation sites mediate binding to 14-3-3 proteins, which sequester and inactivate NEDD4-2 (30, 33). Mutation of these residues effectively renders the NEDD4-2 protein resistant to inhibition by SGK1 (14, 34). Coexpression of L-WNK1 and constitutively active SGK1 S422D with a phosphorylation-resistant double–minor site Nedd4-2 mutant (*Xenopus* Nedd4-2 S338A/T363A; termed NEDD4-2 PR here) decreased steady-state L-WNK1 protein expression, relative to L-WNK1–expressing cells cotransfected with SGK1 and WT NEDD4-2 (Figure 6E). These findings indicate that SGK1 inhibits WNK1 degradation by phosphorylating NEDD4-2 at specific residues previously shown to augment binding to 14-3-3 proteins.
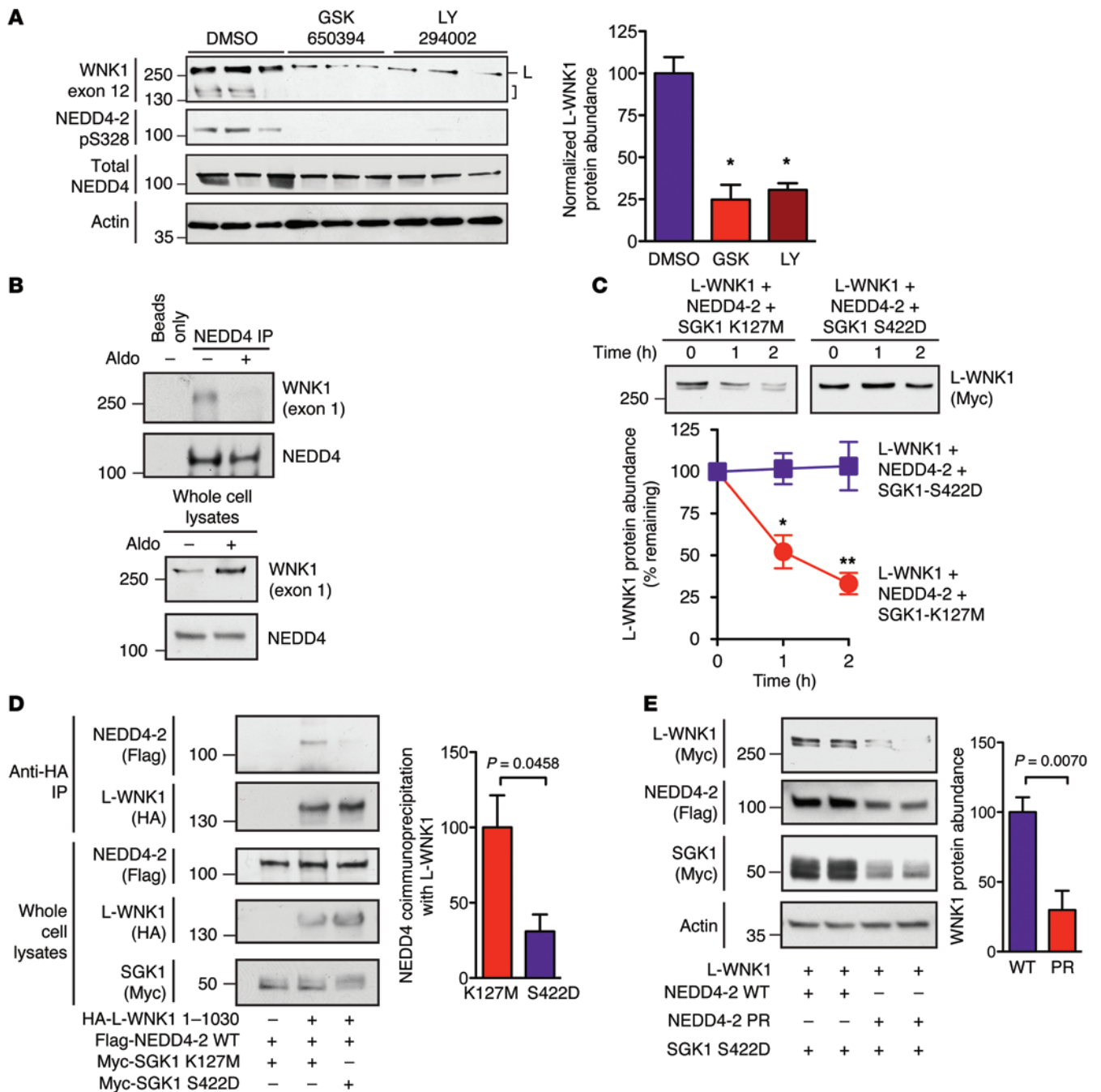
Figure 6. SGK1 attenuates NEDD4-2–mediated WNK1 degradation. (A) Left: mpkCCD$_{c14}$ cells were pretreated with GSK650394 (10 μM), LY294002 (50 μM), or DMSO. Two hours later, cells were stimulated with 100 nM aldosterone for 5 hours and whole cell lysates (20 μg) were subjected to SDS-PAGE and immunoblotting with the indicated antibodies. High-MW signals at approximately 250 kDa, corresponding to L-WNK1 (L) and lower-MW species corresponding to KS-WNK1 and/or proteolytic fragments of L-WNK1 (bracket) are noted. Right: quantification of L-WNK1 abundance. $n = 3$; $P < 0.01$ for either drug vs. DMSO control by 1-way ANOVA, Dunnett's test. **(B)** Co-IP assay in mpkCCD$_{c14}$ cells. Anti–Pan-NEDD4 immunoprecipitates (targeting both NEDD4-1 and NEDD4-2) from cells pretreated with 100 nM aldosterone or vehicle for 14 hours. Representative of 3 experiments. **(C)** HEK-293T cells expressing full-length Myc-tagged L-WNK1 (2 μg/well) and NEDD4-2 (1 μg/well) in the presence of either kinase active SGK1-S422D or dead SGK1-K127M (1 μg/well) were chased with 100 μg CHX for 2 hours. $n = 4$; $P < 0.05$ at 1 hour and $P < 0.01$ at 2 hours by Student's t test. **(D)** Co-IP assay in HEK-293 cells. Anti-HA immunoprecipitates of L-WNK1 1-1030 with NEDD4-2 in the presence of either active (S422D) or kinase dead (K127M) SGK1. $n = 4$; $P = 0.0458$ by Student's t test. **(E)** Steady-state abundance of L-WNK1 transiently expressed in HEK-293T cells with SGK1 S422D and either WT NEDD4-2 or phosphorylation-resistant (PR; S338A/T363A) NEDD4-2. $n = 4$; $P = 0.007$ by Student's t test.

WNK1 is required for the NEDD4-2/SGK1 axis to modulate NCC abundance and phosphorylation status. The observation that NEDD4-2 and SGK1 can control WNK1 abundance suggests that these 2 proteins may exert at least some of their downstream

regulatory effects on NCC via WNK1. To test this hypothesis, we initially attempted simultaneous L-WNK1 knockdown and NCC/NEDD4-2/SGK1 overexpression studies in HEK-293T cells. These experiments were technically challenging, how-
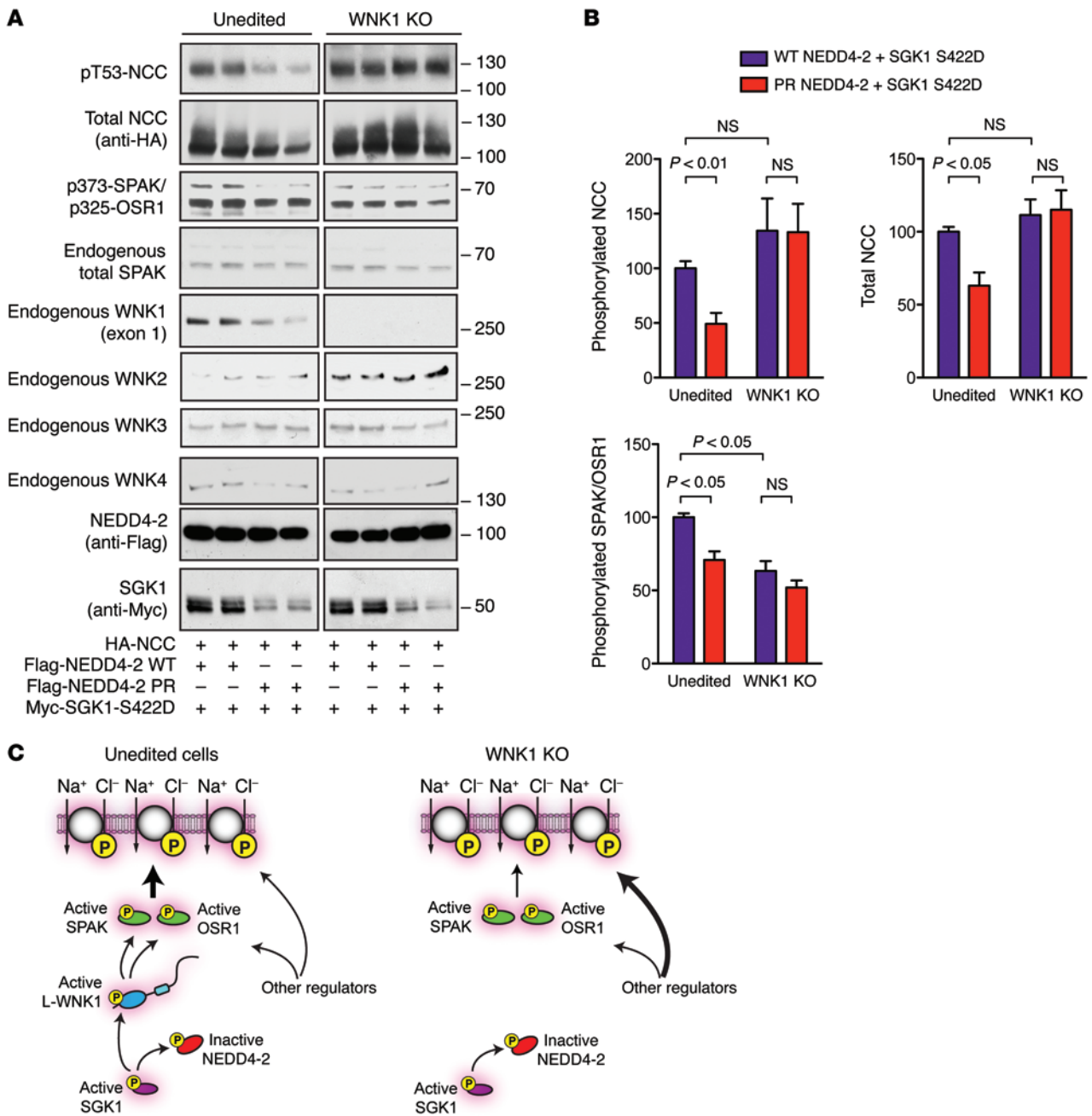
Figure 7. WNK1 is necessary for NEDD4-2 and SGK1 to modulate NCC abundance and phosphorylation in HEK-293 cells. (**A**) *WNK1* KO HEK-293T cells and unedited controls were transfected with NCC (1 μg), SGK1-S422D (1 μg), and either WT or phosphorylation-resistant (PR) NEDD4-2 (1 μg). Thirty-six hours after transfection, the cells were lysed and subjected to immunoblotting with the indicated antibodies. (**B**) Quantification of total NCC, phosphorylated NCC, and phosphorylated SPAK/OSR1 signal in **A**. *n* = 4; *P* values as indicated by 1-Way ANOVA Bonferroni multiple-comparisons post hoc test. (**C**) Proposed model of the effects of *WNK1* deletion on NEDD4-2/SGK1 regulation of NCC in HEK-293T cells. In unedited cells, WT NEDD4-2 interacts with L-WNK1. This interaction can be disrupted by SGK1 phosphorylation at previously defined major and minor sites, increasing L-WNK1 abundance, SPAK/OSR1 phosphorylation, and NCC activation. In *WNK1* KO cells, NEDD4-2 and SGK1 cannot alter NCC phosphorylation status. Other regulators, possibly WNK complexes that are less NEDD4-2 sensitive, maintain NCC activity through compensation.

ever, due to inefficient *WNK1* gene silencing. To overcome this hurdle, we employed CRISPR/Cas-mediated gene-editing technology to generate a *WNK1* KO cell line. These previously validated KO cells completely lack endogenous L-WNK1 protein expression and exhibit reduced native SPAK/OSR1 activity (19). We compared the effect of SGK1 on NCC phosphorylation status in *WNK1* KO cells and paired unedited controls, in the pres-

ence of either WT NEDD4-2 or the SGK1-resistant NEDD4-2 PR mutant. In unedited HEK-293T cells, NCC abundance and phosphorylation status was higher when active SGK1 was coexpressed with WT NEDD4-2, compared with when it was coexpressed with the NEDD4-2 PR mutant (Figure 7, A and B). This is consistent with prior observations that SGK1 can modulate NCC activity through NEDD4-2 phosphorylation (35). The changes in
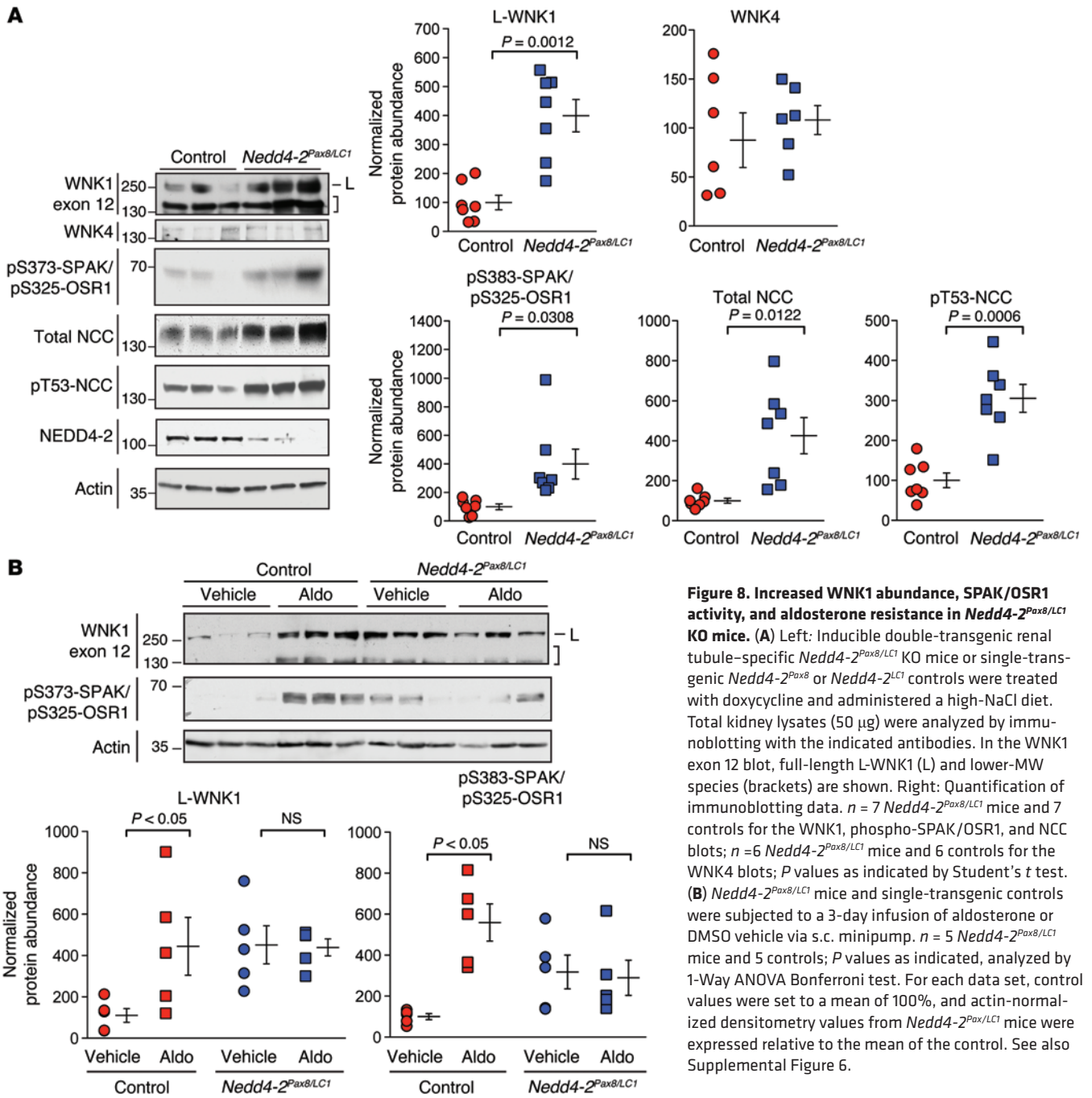
Figure 8. Increased WNK1 abundance, SPAK/OSR1 activity, and aldosterone resistance in *Nedd4-2^Pax8/LC1* **KO mice.** (**A**) Left: Inducible double-transgenic renal tubule–specific *Nedd4-2^Pax8/LC1* KO mice or single-transgenic *Nedd4-2^Pax8* or *Nedd4-2^LC1* controls were treated with doxycycline and administered a high-NaCl diet. Total kidney lysates (50 μg) were analyzed by immunoblotting with the indicated antibodies. In the WNK1 exon 12 blot, full-length L-WNK1 (L) and lower-MW species (brackets) are shown. Right: Quantification of immunoblotting data. *n* = 7 *Nedd4-2^Pax8/LC1* mice and 7 controls for the WNK1, phospho-SPAK/OSR1, and NCC blots; *n* =6 *Nedd4-2^Pax8/LC1* mice and 6 controls for the WNK4 blots; *P* values as indicated by Student's *t* test. (**B**) *Nedd4-2^Pax8/LC1* mice and single-transgenic controls were subjected to a 3-day infusion of aldosterone or DMSO vehicle via s.c. minipump. *n* = 5 *Nedd4-2^Pax8/LC1* mice and 5 controls; *P* values as indicated, analyzed by 1-Way ANOVA Bonferroni test. For each data set, control values were set to a mean of 100%, and actin-normalized densitometry values from *Nedd4-2^Pax/LC1* mice were expressed relative to the mean of the control. See also Supplemental Figure 6.

NCC that were observed in unedited cells were associated with similar changes in SPAK/OSR1 phosphorylation status (Figure 7, A and B), suggesting that signaling through WNK kinases was required for this effect. In *WNK1* KO cells, however, we found that the abundance and phosphorylation status of SPAK/OSR1 and NCC was not altered, regardless of whether active SGK1 was coexpressed with WT NEDD4-2 or the phosphorylation-resistant mutant. Interestingly, though SPAK/OSR1 phosphorylation was decreased in *WNK1* KO cells (Figure 7, A and B), the abundance and phosphorylation status of NCC was not decreased relative to unedited controls, possibly because of compensatory changes in other endogenous WNK kinases within the passage window studied, such as WNK2 or WNK3 (Figure 7, A and C).

In this regard, WNK3 was recently shown to be capable of activating NCC independently of NEDD4-2 and SPAK/OSR1 (36). Alternatively, the NCC activity may have been maintained by other undefined NCC-specific regulators that compensate for the absence of WNK1 activity. Collectively, these findings indicate that aldosterone-regulated interactions between NEDD4-2 and SGK1 are unable to modulate SPAK/OSR1 and NCC activity when WNK1 is absent (Figure 7C). The data therefore implicate WNK1 as a downstream NEDD4-2 substrate that transduces SGK1-dependent signals that regulate NCC, suggesting a molecular mechanism by which aldosterone-regulated signaling intermediates can interface with the WNK-SPAK/OSR1 signaling pathway.
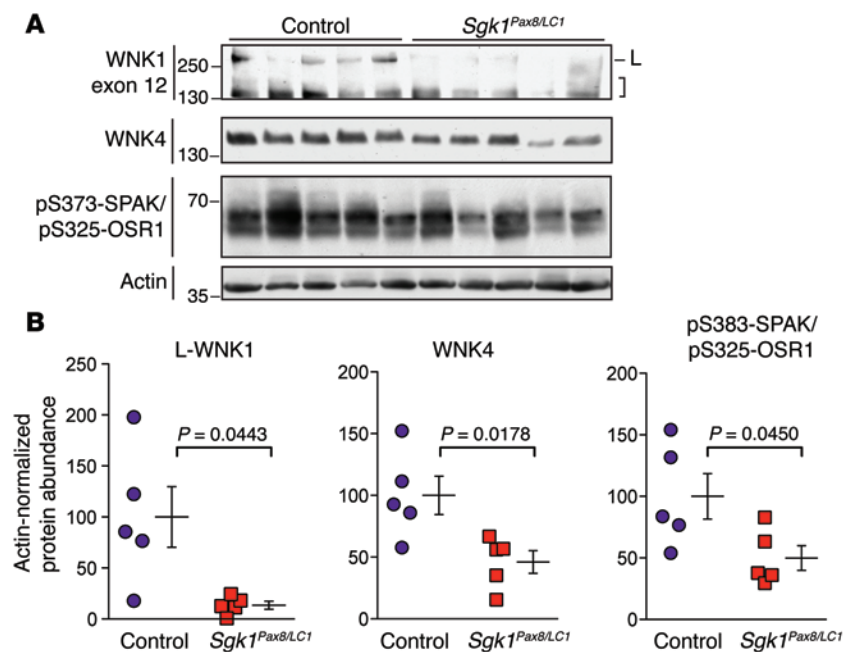
Figure 9. Decreased WNK1 abundance and SPAK/OSR1 activity in *Sgk1^{Pax8/LC1}* KO mice. (**A**) Inducible double-transgenic renal tubule–specific *Sgk1^{Pax8/LC1}* KO mice or single-transgenic *Sgk1^{Pax8}* or *Sgk1^{LC1}* controls were treated with doxycycline and administered a low-NaCl diet. Total kidney lysates (50 μg) were analyzed by immunoblotting with the indicated antibodies. In the WNK1 exon 12 blot, full-length L-WNK1 (L) and lower-MW species (brackets) are shown. *n* = 5 *Sgk1^{Pax8/LC1}* mice and 5 controls; *P* values as indicated, analyzed by Student's *t* test with Welch's correction. (**B**) Quantification of immunoblotting data in **A**. Control values were set to a mean of 100%, and actin-normalized densitometry values from *Sgk1^{Pax8/LC1}* mice were expressed relative to the mean of the control.

Renal tubular NEDD4-2 and SGK1 deficiency exerts opposite effects on WNK1 abundance and downstream SPAK/OSR1 activation. To determine the in vivo relevance of these findings, we analyzed the WNK-SPAK/OSR1 pathway in an inducible renal tubule–specific *Nedd4-2* KO mouse model (*Nedd4-2^{fl/fl} Pax8-rtTA TRE-LC1*, herein referred to as *Nedd4-2^{Pax8/LC1}*; ref. 37). These mice are homozygous for a floxed *Nedd4-2* allele, bred into double-transgenic mice that express tetracycline-inducible Cre recombinase selectively in renal tubules. Administering doxycycline to these animals enables Cre-mediated excision of the loxP-flanked region, resulting in postdevelopmental *Nedd4-2* ablation. On a high-NaCl diet, *Nedd4-2^{Pax8/LC1}* mice exhibit increased NCC activity relative to controls, despite suppressed aldosterone levels. Consistent with our observations in cell-culture systems, we found that the expression of exon 12–containing WNK1 isoforms was increased in double-transgenic *Nedd4-2^{Pax8/LC1}* mice, relative to single-transgenic controls (Figure 8A and Supplemental Figure 6A). The 250 kDa L-WNK1 species was strongly increased, and this was associated with enhanced S-motif phosphorylation of SPAK/OSR1, a signature of WNK-mediated activation (38). Total and phosphorylated NCC was also significantly increased, consistent with prior reports (37). Using a C-terminal SPAK antibody (38), we were unable to detect a qualitative directional shift in the expression of previously described long and short SPAK isoforms in *Nedd4-2* KO mice (Supplemental Figure 6A; refs. 39, 40), and in contrast to WNK1, we saw no significant difference in WNK4 abundance between control and KO groups. Collectively, these findings support the in vitro observations that NEDD4-2 negatively regulates WNK1 abundance. Though the ablation of NEDD4-2 in renal tubules could potentially augment NCC activity via multiple mechanisms, these data are consistent with the view that *Nedd4-2* deletion activates NCC, at least in part by increasing L-WNK1 protein abundance and downstream SPAK/OSR1 phosphorylation.

We also tested the effect of aldosterone infusion on WNK1 protein abundance in *Nedd4-2* KO mice. In these studies, control and KO animals were subjected to aldosterone infusion or vehicle

via s.c. implanted minipump over 3 days. In control single-transgenic animals with intact NEDD4-2 expression, aldosterone infusion increased the protein abundance of WNK1 significantly, relative to vehicle-treated animals (Figure 8B and Supplemental Figure 6B). Consistent with a net increase in L-WNK1 kinase activity, downstream SPAK/OSR1 phosphorylation was increased in control mice. In contrast, *Nedd4-2^{Pax8/LC1}* animals exhibited high WNK1 exon 12 isoform expression at baseline, and aldosterone did not increase the abundance of these WNK1 isoforms further, suggesting that aldosterone induces WNK1 protein expression in vivo via NEDD4-2 inhibition.

To further evaluate how the NEDD4-2/SGK1 axis influences WNK1 protein expression in vivo, we also analyzed WNK1 protein abundance in *Sgk1^{Pax8/LC1}* KO mice (*Sgk1^{fl/fl} Pax8-rtTA TRE-LC1*), the corresponding tet-inducible renal tubule–specific KO model that lacks SGK1 expression. Previous studies have shown that these mice exhibit a phenotype that is a mirror image to that of *Nedd4-2^{Pax8/LC1}* KOs; i.e., when subjected to a low-NaCl diet, *Sgk1^{Pax8/LC1}* mice develop relative salt wasting, reduced blood pressure, and elevated aldosterone levels compared with controls (41). These effects are associated with low NCC expression and reduced NEDD4-2 major-site phosphorylation. Because our data suggest that WNK1 acts as a downstream intermediary between NEDD4-2 and NCC, we reasoned that *Sgk1^{Pax8/LC1}* mice should exhibit low WNK1 protein abundance, compared with controls, when placed under dietary conditions that promote aldosterone secretion. Consistent with this, we found that *Sgk1^{Pax8/LC1}* mice placed on an NaCl-restricted diet (<0.1% NaCl for 7 days) exhibited significantly lower WNK1 exon 12 isoform abundance compared with single-transgenic controls subjected to the same dietary maneuver (Figure 9, A and B). WNK4 abundance was also significantly lower in these mice, possibly due to known direct interactions between SGK1, WNK1, and WNK4 (42–44). Consistent with decreased WNK1 and WNK4 kinase activity, downstream SPAK/OSR1 phosphorylation was also reduced (Figure 9, A and B). Taken together,
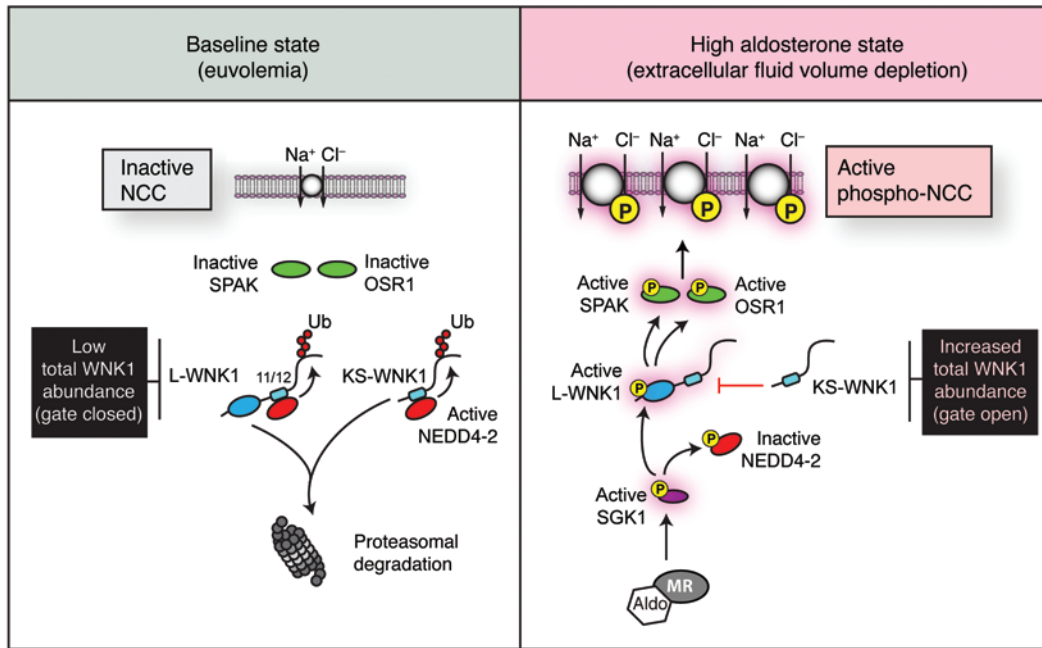
Figure 10. Model of aldosterone-mediated activation of SPAK/OSR1 and NCC via WNK1. In the baseline euvolemic state, active NEDD4-2 binds to the PY motifs in exons 11 and 12 of WNK1, ubiquitylating the WNK1 C-terminus and targeting it for proteasomal degradation. This limits total WNK1 protein expression, acting as a closed gate that shuts off downstream SPAK/OSR1 and NCC activity. During states where aldosterone levels are high, such as extracellular fluid volume depletion, SPAK and OSR1 are phosphorylated and active. Aldosterone contributes to this process by driving the transcription of *SGK1* in the distal nephron. Active SGK1 phosphorylates and inactivates NEDD4-2, reducing its interaction with exons 11 and 12 of WNK1. This opens the gate, increasing total WNK1 protein expression. Once WNK1 protein is present, SGK1 can directly phosphorylate the N-terminus of L-WNK1, resulting in selective L-WNK1 activation (43). Active L-WNK1 then stimulates SPAK and OSR1 to directly phosphorylate NCC. Previous data suggest that the SGK1 pathway may be particularly active during states that require the conservation of sodium (59, 68). Other stimuli for aldosterone secretion, such as hyper-kalemia, may selectively upregulate KS-WNK1 protein expression via additional undefined mechanisms to attenuate L-WNK1 and NCC activity (55, 59, 60). Such effects may act in concert with changes in intracellular [Cl−] to suppress WNK activity (61). Additionally, other SGK1-dependent effects on NCC, including suppression of WNK4-mediated NCC degradation (46) or ubiquitylation of NCC by NEDD4-2 (35), are not shown here to highlight the mechanism of SPAK/OSR1 activation described in this study.

data from these mouse models support the idea that aldosterone stimulates WNK1 protein expression via SGK1-dependent inhibition of NEDD4-2, and that the net effect of this regulatory interaction results in enhanced downstream SPAK/OSR1 phosphorylation and NCC activation.

Discussion

All members of the WNK kinase family are large proteins that possess a complex multidomain architecture, suggesting that they integrate signals from a variety of inputs to mediate their downstream effects (45). A major function of WNKs is to act as penultimate kinases in phosphorylation-dependent signaling cascades that activate sodium-coupled cation chloride cotransporters. Although SPAK and OSR1 have been identified as the 2 downstream effectors that directly catalyze cotransporter phosphorylation, the upstream molecular events that connect physiological stimuli to the WNKs are poorly understood. Here, we have defined a mechanism that explains how signals transduced from the MR can interface with the renal WNK signaling pathway to trigger SPAK and OSR1 activation. The mechanism involves an aldosterone-regulated interaction between the E3 ubiquitin ligase NEDD4-2 and WNK1. Our data show that NEDD4-2 associates with WNK1 via PY motifs harbored within 2 alternatively spliced proline-rich exons that are present in kidney-expressed WNK1

isoforms. Upon binding, NEDD4-2 destabilizes WNK1, targeting it for degradation via the ubiquitin proteasome pathway. The aldosterone-induced kinase SGK1 attenuates this process through the phosphorylation of specific residues that suppress NEDD4-2 function. In a model cell line lacking WNK1 protein expression, NEDD4-2 and SGK1 lose their ability to modulate NCC, suggesting that WNK1 plays an essential role in aldosterone-mediated NCC activation. Consistent with this idea, WNK1 protein expression is high and resistant to aldosterone infusion in *Nedd4-2* KO mice and low in mice that lack SGK1, prompting opposite effects on downstream SPAK/OSR1 and NCC activation. Together, these observations delineate a mechanism by which aldosterone can increase the abundance of a specific WNK kinase in the ASDN, leading to the stimulation of signaling cascades that enhance NCC activity and distal salt reabsorption.

Previous studies have suggested that aldosterone can stimulate NCC trafficking and plasma membrane expression via 2 distinct mechanisms that require SGK1. Overexpression of WT WNK4 inhibits NCC surface delivery from the trans-Golgi network; SGK1 impedes this process by directly phosphorylating residues in the WNK4 C-terminus (46). More recently, a study found that NEDD4-2 ubiquitylates and downregulates NCC surface expression in a manner that can be reversed by SGK1, suggesting a more direct mechanism by which NEDD4-2 can regulate NCC turnover

(35). Although NEDD4-2 and NCC formed complexes that could be disrupted by SGK1, the exact nature of the interaction remains undefined, as NCC contains no canonical PY motif. Nevertheless, NCC protein abundance is strongly increased in *Nedd4-2* KO mice (37), implicating an important role for NEDD4-2–mediated ubiquitylation of NCC in blood-pressure regulation. Both of these reports potentially explain how aldosterone can posttranslationally alter the abundance of NCC through effects on protein trafficking. However, other studies have suggested that aldosterone also stimulates distal sodium transport via SPAK and OSR1 (6, 47). Thus, aldosterone must somehow signal through WNK kinases to regulate SPAK/OSR1-mediated NCC activation. The data presented here suggest that WNK1 is required for this effect, since WNK1 ablation in cells negates the ability of NEDD4-2 and SGK1 to modulate SPAK/OSR1 and NCC phosphorylation, and in vivo studies indicate that aldosterone can activate SPAK/OSR1 by altering WNK1 protein expression and activity.

Our analyses confirm prior observations that total NCC protein abundance is increased in *Nedd4-2*$^{Pax8/LC1}$ KO mice, relative to NEDD4-2–intact controls. We also observed a comparable increase in the abundance of phosphorylated NCC, consistent with previous reports that the phosphorylated-to-total NCC ratios between controls and *Nedd4-2* KO animals are similar (37). At first glance, this result may seem at odds with the increase in SPAK/OSR1 phosphorylation seen in *Nedd4-2* KO mice. An important issue to consider, however, is the observation that *Nedd4-2*$^{Pax8/LC1}$ mice are hypoaldosteronemic, relative to controls. Since these mice are hypertensive from disinhibition of NCC activity, the low aldosterone levels are consistent with feedback suppression due to extracellular fluid volume expansion. If NEDD4-2 ablation solely mediated this effect by way of a pure effect on cotransporter trafficking, the increased number of NCC molecules at the plasma membrane would be expected to downregulate SPAK and OSR1 activity, and decrease the phosphorylated-to-total NCC ratio due to negative feedback. Clearly, this was not observed in our studies, since we detected an increase in WNK1 abundance and a corresponding increase in SPAK/OSR1 phosphorylation status (Figure 8). It is possible that the lack of change in the phosphorylated-to-total NCC ratio could be due an unidentified compensatory factor that attenuates NCC phosphorylation status in response to volume expansion, such as a phosphatase. The catalytic activity of such a factor might partially mitigate enhanced SPAK/OSR1 activity, resulting in normalization of the phosphorylated-to-total NCC ratio. Indeed, previous work indicates that cation-chloride cotransporters such as NCC can be dephosphorylated (48), and recent studies suggest that such mechanisms may be highly relevant to NCC regulation in vivo (49).

Given the importance of the WNK signaling pathway in the fine-tuning of electrolyte balance (1), the stability of WNK kinases is likely tightly controlled. One key regulator is the KLHL3/CUL3 RING E3 ubiquitin ligase complex, which ubiquitylates and degrades WNK1 and WNK4 (50–52). Mutations of this complex cause FHHt by impairing its ability to dispose of WNK1 and WNK4, either through reduced binding of WNK1 and WNK4 to the KLHL3 adaptor (51) or by CUL3 exon-skipping mutations that augment ubiquitylation and degradation of KLHL3 (53). Given the fact, however, that this E3 ligase complex regulates more than one

WNK, other mechanisms must be in place to modulate WNK complex composition and stoichiometry. Here, we identify NEDD4-2 as an E3 ligase that interacts with a specific WNK kinase through a defined, aldosterone-regulated signaling mechanism. Notably, the canonical PY motifs in WNK1 are unique among kidney-expressed WNKs and therefore provide a distinctive binding site for NEDD4-2. Since this E3 ligase is tightly regulated by SGK1, the interaction provides a mechanism by which aldosterone can specifically access and activate the WNK signaling pathway through rapid SGK1 induction. Moreover, the functional PY motifs are the only 2 such motifs contained within the entire WNK1 sequence and are tightly restricted to the same proline-rich region of the protein, within 2 neighboring exons that undergo extensive tissue-specific alternative splicing. Therefore, they reside within an adaptable domain that can change, depending on the physiological requirements of a specific cell type or tissue. WNK1 has been implicated in a variety of processes outside of epithelial ion transport, including cell growth and differentiation, cardiovascular development, and neuronal function (44). Thus, regulated splicing of these proline-rich cassettes may be a mechanism by which cells can limit the diverse actions of WNK1 to a specific subset of operations, independently of KLHL3 and CUL3 regulation.

Previous work has established that L-WNK1 can function as an upstream SGK1 activator (54). In contrast to those results, we report here that NEDD4-2 negatively regulates WNK1 abundance and that this effect can be blocked by SGK1. Therefore, our data identify WNK1 as a downstream SGK1 target. Although these findings may seem contradictory, they can be explained by key structural differences in the *WNK1* cDNAs that were used in each of the studies. Notably, all of the experiments that had identified SGK1 as an L-WNK1 target were conducted with either N-terminal L-WNK1 fragments or an L-WNK1 Δ11/12 splice variant lacking PY motifs. Thus, in those studies, the signaling pathway that was characterized was one in which NEDD4-2 interaction was minimized. Once the proline-rich cassettes were incorporated into L-WNK1, the kinase became a robust NEDD4-2 substrate whose abundance could be upregulated by SGK1, thus placing WNK1 downstream of SGK1 action. Collectively, these data suggest that splicing of exons 11 and 12 into the WNK1 sequence reorients the molecular relationship between WNK1, NEDD4-2, and SGK1 in aldosterone-sensitive tissues. As shown in this study and by others (10), WNK1 isoforms containing proline-rich cassettes are highly represented in the ASDN. Therefore, the pattern of *WNK1* gene expression in the distal nephron positions WNK1 downstream of SGK1, with NEDD4-2 being an intermediary that suppresses WNK1 protein abundance in the absence of aldosterone. Previous observations that SGK1 directly phosphorylates and activates L-WNK1 through interactions with its N-terminus further support the notion that WNK1 functions downstream of SGK1 in the ASDN (43). Thus, during high aldosterone states, NEDD4-2 inhibition would be expected to increase WNK1 protein abundance, expanding the supply of L-WNK1 kinases that can be activated by SGK1 and trigger downstream signaling through SPAK and OSR1 (Figure 10).

The balance of L-WNK1 and KS-WNK1 isoforms has been proposed to function as a molecular switch that coordinates NaCl reabsorption and K$^+$ secretion in the distal nephron (55). With regards to NCC regulation, L-WNK1 is a stimulator (28, 56), while KS-WNK1

is an inhibitor that suppresses the catalytic activity of several WNK kinases (57, 58). We found that exons 11 and 12 are represented in both L-WNK1 and KS-WNK1 in human kidney tissue and that NEDD4-2 ubiquitylates the C-terminus common to both isoforms. Thus, aldosterone would be expected to increase the abundance of WNK1 isoforms that exert stimulatory and inhibitory effects toward NCC. Analyses of WNK1 protein expression indeed suggested this, since both L-WNK1 and lower-MW WNK1 species were induced by aldosterone (Figure 3). The net effect of this increase in total WNK1 expression, however, appeared to result in enhanced L-WNK1 activity, since SPAK/OSR1 phosphorylation was increased in aldosterone-treated mpkCCD$_{c14}$ cells and in *Nedd4-2* KO mice (Figure 3 and Figure 8). Since our data suggest that the protein abundance of both L- and KS-WNK1 are increased in the presence of aldosterone, one potential role of the proline-rich cassettes may be to increase total WNK1 availability during high aldosterone states. In other words, NEDD4-2 could function as a regulated gate that interacts with the PY motifs in WNK1, shutting off WNK1-dependent signaling processes in the absence of aldosterone (Figure 10). By analogy, an increase in circulating aldosterone levels would open the gate via SGK1, inactivating NEDD4-2 and increasing the total number of WNK1 isoforms that are available for regulation. As reported previously, once total WNK1 protein expression is increased, active SGK1 could then selectively phosphorylate the N-terminus of L-WNK1, turning on its kinase activity (Figure 10; ref. 43). As proposed by several groups (1, 46, 59, 60), the relative balance of L-WNK1 and KS-WNK1 might then be further adjusted by other factors that specifically tune the effects of aldosterone to favor renal K$^+$ secretion or sodium chloride reabsorption, depending on the physiologic circumstance. These effects would likely work in synergy with direct effects of extracellular potassium on basolateral membrane voltage, intracellular chloride, and L-WNK1 kinase activity in the distal nephron (61).

Though aldosterone has traditionally been viewed as the canonical natural inhibitor of NEDD4-2 function, insulin and vasopressin can also trigger the expression and activity of specific kinases that inhibit NEDD4-2 via mechanisms that are identical to SGK1. Furthermore, emerging data indicate that, like aldosterone, insulin and vasopressin also trigger SPAK/OSR1-mediated NCC phosphorylation (7, 38). Since changes in WNK1 protein abundance are directly linked to SPAK and OSR1 activity, our findings suggest that aldosterone, insulin, and vasopressin could all potentially leverage the interaction between NEDD4-2 and WNK1 as a means to activate NCC. Thus, the results presented here potentially explain how diverse hormonal signaling pathways could converge upon a specific WNK kinase to regulate salt transport and blood pressure.

Methods

Molecular methods. All L-WNK1 clones used in this study were derived from the original rat L-*Wnk1* cDNA, isolated from rat forebrain (24) and were generated as described in the Supplemental Methods.

Exon 12 antibody. The WNK1 exon 12 antisera were generated by immunizing rabbits to a keyhole limpet hemocyanin–conjugated peptide epitope located within exon 12 of rat WNK1 (SQPAVSLSQQPPTTSSQQC). Peptide synthesis, production of rabbit antisera, and peptide affinity purification were performed by Abgent.

Cell culture and transfection. HEK-293T cell culture and transfection protocols were carried out as described previously (62). Cells were analyzed 24–48 hours after transfection. Mouse CCD (mpkCCD$_{c14}$) cells were cultured using previously established protocols (18). For analyses of aldosterone response, mpkCCD$_{c14}$ cells were grown to confluence in 6-well dishes and were cultured in basic medium lacking hormones 24 hours prior to incubation.

Preparation of lysates and immunoblot analysis. Immunoblot analysis was performed as described previously (62). Freshly dissected kidneys were flash frozen prior to analysis, and homogenates were prepared as described (63). Typically, 50–100 μg protein were analyzed by immunoblotting of kidney lysates.

RNAi studies. Transient siRNA-mediated knockdown of NEDD4 isoforms in HEK-293T cells was performed as described in the Supplemental Methods.

Assays to monitor L-WNK1 degradation. CHX chase assays in HEK-293T cells were carried out as described previously (62). For chase assays in the presence of the proteasome inhibitor MG-132, transiently transfected cells were pretreated with 10 μM MG-132 or DMSO vehicle control for 4 hours, prior to the initiation of the chase.

In vivo ubiquitylation assay. HaloLink resin pulldowns (Promega) were employed to analyze NEDD4-2–mediated ubiquitylation of the WNK1 N- and C-termini in HEK-293T cells, as described in detail in the Supplemental Methods.

Coimmunoprecipitation studies. Coimmunoprecipitation studies in HEK-293T and mpkCCD$_{c14}$ cells were performed with antibody-conjugated resins or protein A/G agarose, as described (62).

Transcript analysis. RT-PCR studies in human kidney, and qPCR studies in mpkCCD$_{c14}$ cells were carried out as described in the Supplemental Methods.

Immunofluorescence microscopy. Cryosectioning, blocking, and immunostaining of kidney sections from adult Sprague-Dawley rats was performed as described previously (64). Sections were mounted with Vectashield (Vector Laboratories) and examined using a Leica TCS SP5 confocal microscope.

Animal studies. Tetracycline inducible, nephron-specific *Nedd4-2*[Pax8/LC1] KO mice (*Nedd4-2*^{fl/fl} *Pax8-rtTA TRE-LC1*) and *Sgk1*[Pax8/LC1] KO mice (*Sgk1*^{fl/fl} *Pax8-rtTA TRE-LC1*) were studied using previously described protocols (37, 41), described in detail in the Supplemental Methods.

Statistics. Quantification of Western blots was carried out using NIH ImageJ software. Statistical analysis was performed using Graph-Pad Prism software. Measurements are presented as mean ± SEM. Comparisons between 2 groups were analyzed by unpaired 2-tailed Student's or Welch *t* tests. Multiple comparisons were performed by *t* tests with Bonferroni correction or by 1-way ANOVA followed by the appropriate post hoc tests, as indicated. qPCR data were analyzed by Kruskal-Wallis nonparametric 1-way ANOVA, followed by Dunn's multiple comparison post hoc test. A base *P* value of <0.05 was considered statistically significant. Quantification of endogenous WNK1 signal was limited to L-WNK1–specific bands (>250 kDa) that were detected with the exon 12 antibody. We refrained from quantifying lower-MW species <250 kDa, as short KS-WNK1 isoforms could not be reliably distinguished from proteolytically processed WNK1 fragments.

Study approval. All animal protocols were approved by the IACUC at the University of Pittsburgh School of Medicine, or by the Swiss Federal Veterinary Office, and carried out in accordance to the animal welfare act.

Address correspondence to: Arohan R. Subramanya, Department of Medicine, Renal-Electrolyte Division, University of Pittsburgh School of Medicine, S828A Scaife Hall, 3550 Terrace Street, Pittsburgh, Pennsylvania 15261, USA. Phone: 412.624.3669; E-mail: ars129@pitt.edu.

1. Welling PA, Chang YP, Delpire E, Wade JB. Multigene kinase network, kidney transport, and salt in essential hypertension. *Kidney Int*. 2010;77(12):1063–1069.

2. Subramanya AR, Ellison DH. Distal convoluted tubule. *Clin J Am Soc Nephrol*. 2014;9(12):2147–2163.

3. Vitari AC, Deak M, Morrice NA, Alessi DR. The WNK1 and WNK4 protein kinases that are mutated in Gordon's hypertension syndrome phosphorylate and activate SPAK and OSR1 protein kinases. *Biochem J*. 2005;391(pt 1):17–24.

4. Moriguchi T, et al. WNK1 regulates phosphorylation of cation-chloride-coupled cotransporters via the STE20-related kinases, SPAK and OSR1. *J Biol Chem*. 2005;280(52):42685–42693.

5. Castaneda-Bueno M, et al. Activation of the renal Na^+:Cl^- cotransporter by angiotensin II is a WNK4-dependent process. *Proc Natl Acad Sci U S A*. 2012;109(20):7929–7934.

6. Chiga M, et al. Dietary salt regulates the phosphorylation of OSR1/SPAK kinases and the sodium chloride cotransporter through aldosterone. *Kidney Int*. 2008;74(11):1403–1409.

7. Komers R, et al. Enhanced phosphorylation of $Na(+)$-Cl^- co-transporter in experimental metabolic syndrome: role of insulin. *Clin Sci (Lond)*. 2012;123(11):635–647.

8. Pedersen NB, Hofmeister MV, Rosenbaek LL, Nielsen J, Fenton RA. Vasopressin induces phosphorylation of the thiazide-sensitive sodium chloride cotransporter in the distal convoluted tubule. *Kidney Int*. 2010;78(2):160–169.

9. Pearce D. SGK1 regulation of epithelial sodium transport. *Cell Physiol Biochem*. 2003;13(1):13–20.

10. Vidal-Petiot E, et al. A new methodology for quantification of alternatively spliced exons reveals a highly tissue-specific expression pattern of WNK1 isoforms. *PLoS One*. 2012;7(5):e37751.

11. Delaloy C, et al. Multiple promoters in the WNK1 gene: one controls expression of a kidney-specific kinase-defective isoform. *Mol Cell Biol*. 2003;23(24):9208–9221.

12. Chen HI, Sudol M. The WW domain of Yes-associated protein binds a proline-rich ligand that differs from the consensus established for Src homology 3-binding modules. *Proc Natl Acad Sci U S A*. 1995;92(17):7819–7823.

13. Staub O, et al. WW domains of Nedd4 bind to the proline-rich PY motifs in the epithelial Na^+ channel deleted in Liddle's syndrome. *EMBO J*. 1996;15(10):2371–2380.

14. Debonneville C, et al. Phosphorylation of Nedd4-2 by Sgk1 regulates epithelial $Na(+)$ channel cell surface expression. *EMBO J*. 2001;20(24):7052–7059.

15. Kanelis V, Bruce MC, Skrynnikov NR, Rotin D, Forman-Kay JD. Structural determinants for high-affinity binding in a Nedd4 WW3* domain-Comm PY motif complex. *Structure*. 2006;14(3):543–553.

16. Rinehart J, et al. WNK2 kinase is a novel regulator of essential neuronal cation-chloride cotransporters. *J Biol Chem*. 2011;286(34):30171–30180.

17. O'Reilly M, Marshall E, Speirs HJ, Brown RW. WNK1, a gene within a novel blood pressure control pathway, tissue-specifically generates radically different isoforms with and without a kinase domain. *J Am Soc Nephrol*. 2003;14(10):2447–2456.

18. Bens M, et al. Corticosteroid-dependent sodium transport in a novel immortalized mouse collecting duct principal cell line. *J Am Soc Nephrol*. 1999;10(5):923–934.

19. Roy A, et al. Generation of WNK1 KO cell lines by CRISPR/Cas-mediated genome editing. *Am J Physiol Renal Physiol*. 2015;308(4):F366–F376.

20. Elvira-Matelot E, et al. Regulation of WNK1 expression by miR-192 and aldosterone. *J Am Soc Nephrol*. 2010;21(10):1724–1731.

21. Naray-Fejes-Toth A, Snyder PM, Fejes-Toth G. The kidney-specific WNK1 isoform is induced by aldosterone and stimulates epithelial sodium channel-mediated Na^+ transport. *Proc Natl Acad Sci U S A*. 2004;101(50):17434–17439.

22. O'Reilly M, et al. Dietary electrolyte-driven responses in the renal WNK kinase pathway in vivo. *J Am Soc Nephrol*. 2006;17(9):2402–2413.

23. Pak Y, Glowacka WK, Bruce MC, Pham N, Rotin D. Transport of LAPTM5 to lysosomes requires association with the ubiquitin ligase Nedd4, but not LAPTM5 ubiquitination. *J Cell Biol*. 2006;175(4):631–645.

24. Xu B, English JM, Wilsbacher JL, Stippec S, Goldsmith EJ, Cobb MH. WNK1, a novel mammalian serine/threonine protein kinase lacking the catalytic lysine in subdomain II. *J Biol Chem*. 2000;275(22):16795–16801.

25. Kanelis V, Rotin D, Forman-Kay JD. Solution structure of a Nedd4 WW domain-ENaC peptide complex. *Nat Struct Biol*. 2001;8(5):407–412.

26. Abriel H, et al. Defective regulation of the epithelial Na^+ channel by Nedd4 in Liddle's syndrome. *J Clin Invest*. 1999;103(5):667–673.

27. Radivojac P, et al. Identification, analysis, and prediction of protein ubiquitination sites. *Proteins*. 2010;78(2):365–380.

28. Chavez-Canales M, et al. WNK-SPAK-NCC cascade revisited: WNK1 stimulates the activity of the Na-Cl cotransporter via SPAK, an effect antagonized by WNK4. *Hypertension*. 2014;64(5):1047–1053.

29. Wang X, Herr RA, Chua WJ, Lybarger L, Wiertz EJ, Hansen TH. Ubiquitination of serine, threonine, or lysine residues on the cytoplasmic tail can induce ERAD of MHC-I by viral E3 ligase mK3. *J Cell Biol*. 2007;177(4):613–624.

30. Chandran S, et al. Neural precursor cell-expressed developmentally down-regulated protein 4-2 (Nedd4-2) regulation by 14-3-3 protein binding at canonical serum and glucocorticoid kinase 1 (SGK1) phosphorylation sites. *J Biol Chem*. 2011;286(43):37830–37840.

31. Kobayashi T, Deak M, Morrice N, Cohen P. Characterization of the structure and regulation of two novel isoforms of serum- and glucocorticoid-induced protein kinase. *Biochem J*. 1999;344(pt 1):189–197.

32. Hallows KR, et al. Phosphopeptide screen uncovers novel phosphorylation sites of Nedd4-2 that potentiate its inhibition of the epithelial Na^+ channel. *J Biol Chem*. 2010;285(28):21671–21678.

33. Bhalla V, et al. Serum- and glucocorticoid-regulated kinase 1 regulates ubiquitin ligase neural precursor cell-expressed, developmentally down-regulated protein 4-2 by inducing interaction with 14-3-3. *Mol Endocrinol*. 2005;19(12):3073–3084.

34. Snyder PM, Olson DR, Kabra R, Zhou R, Steines JC. cAMP and serum and glucocorticoid-inducible kinase (SGK) regulate the epithelial $Na(+)$ channel through convergent phosphorylation of Nedd4-2. *J Biol Chem*. 2004;279(44):45753–45758.

35. Arroyo JP, et al. Nedd4-2 modulates renal Na^+-Cl^- cotransporter via the aldosterone-SGK1-Nedd4-2 pathway. *J Am Soc Nephrol*. 2011;22(9):1707–1719.

36. Lagnaz D, et al. WNK3 abrogates the NEDD4-2-mediated inhibition of the renal Na^+-Cl^- cotransporter. *Am J Physiol Renal Physiol*. 2014;307(3):F275–F286.

37. Ronzaud C, et al. Renal tubular NEDD4-2 deficiency causes NCC-mediated salt-dependent hypertension. *J Clin Invest*. 2013;123(2):657–665.

38. Saritas T, et al. SPAK differentially mediates vasopressin effects on sodium cotransporters. *J Am Soc Nephrol*. 2013;24(3):407–418.

39. McCormick JA, et al. A SPAK isoform switch modulates renal salt transport and blood pressure. *Cell Metab*. 2011;14(3):352–364.

40. Grimm PR, et al. SPAK isoforms and OSR1 regulate sodium-chloride co-transporters in a nephron-specific manner. *J Biol Chem*. 2012;287(45):37673–37690.

41. Faresse N, et al. Inducible kidney-specific Sgk1 KO mice show a salt-losing phenotype. *Am J Physiol Renal Physiol*. 2012;302(8):F977–F985.

42. Rozansky DJ, et al. Aldosterone mediates activation of the thiazide-sensitive Na-Cl cotransporter through an SGK1 and WNK4 signaling pathway. *J Clin Invest*. 2009;119(9):2601–2612.

43. Cheng CJ, Huang CL. Activation of PI3-kinase stimulates endocytosis of ROMK via Akt1/SGK1-dependent phosphorylation of WNK1. *J Am Soc Nephrol*. 2011;22(3):460–471.

44. McCormick JA, Ellison DH. The WNKs: atypical protein kinases with pleiotropic actions. *Physiol Rev*. 2011;91(1):177–219.

45. Richardson C, Alessi DR. The regulation of salt transport and blood pressure by the WNK-SPAK/OSR1 signalling pathway. *J Cell Sci*. 2008;121(pt 20):3293–3304.

46. Rozansky DJ, et al. Aldosterone mediates activation of the thiazide-sensitive Na-Cl cotransporter through an SGK1 and WNK4 signaling pathway. *J Clin Invest*. 2009;119(9):2601–2612.

47. Ko B, et al. Aldosterone acutely stimulates NCC activity via a SPAK-mediated pathway. *Am J Physiol Renal Physiol*. 2013;305(5):F645–F652.

48. Glover M, Mercier Zuber A, Figg N, O'Shaughnessy KM. The activity of the thiazide-sensitive Na(+)-Cl(–) cotransporter is regulated by protein phosphatase PP4. *Can J Physiol Pharmacol*. 2010;88(10):986–995.

49. Sorensen MV, et al. Rapid dephosphorylation of the renal sodium chloride cotransporter in response to oral potassium intake in mice. *Kidney Int*. 2013;83(5):811–824.

50. Ohta A, et al. The CUL3-KLHL3 E3 ligase complex mutated in Gordon's hypertension syndrome interacts with and ubiquitylates WNK isoforms: disease-causing mutations in KLHL3 and WNK4 disrupt interaction. *Biochem J*. 2013;451(1):111–122.

51. Wakabayashi M, et al. Impaired KLHL3-mediated ubiquitination of WNK4 causes human hypertension. *Cell Rep*. 2013;3(3):858–868.

52. Shibata S, Zhang J, Puthumana J, Stone KL, Lifton RP. Kelch-like 3 and Cullin 3 regulate electrolyte homeostasis via ubiquitination and degradation of WNK4. *Proc Natl Acad Sci U S A*. 2013;110(19):7838–7843.

53. McCormick JA, et al. Hyperkalemic hypertension-associated cullin 3 promotes WNK signaling by degrading KLHL3. *J Clin Invest*. 2014;124(11):4723–4736.

54. Xu BE, et al. WNK1 activates SGK1 to regulate the epithelial sodium channel. *Proc Natl Acad Sci U S A*. 2005;102(29):10315–10320.

55. Wade JB, et al. WNK1 kinase isoform switch regulates renal potassium excretion. *Proc Natl Acad Sci U S A*. 2006;103(22):8558–8563.

56. Vidal-Petiot E, et al. WNK1-related Familial Hyperkalemic Hypertension results from an increased expression of L-WNK1 specifically in the distal nephron. *Proc Natl Acad Sci U S A*. 2013;110(35):14366–14371.

57. Subramanya AR, Yang CL, Zhu X, Ellison DH. Dominant-negative regulation of WNK1 by its kidney-specific kinase-defective isoform. *Am J Physiol Renal Physiol*. 2006;290(3):F619–F624.

58. Yang CL, Zhu X, Ellison DH. The thiazide-sensitive Na-Cl cotransporter is regulated by a WNK kinase signaling complex. *J Clin Invest*. 2007;117(11):3403–3411.

59. Vallon V. Regulation of the Na+-Cl- cotransporter by dietary NaCl: a role for WNKs, SPAK, OSR1, and aldosterone. *Kidney Int*. 2008;74(11):1373–1375.

60. Lazrak A, Liu Z, Huang CL. Antagonistic regulation of ROMK by long and kidney-specific WNK1 isoforms. *Proc Natl Acad Sci U S A*. 2006;103(5):1615–1620.

61. Terker AS, et al. Potassium modulates electrolyte balance and blood pressure through effects on distal cell voltage and chloride. *Cell Metab*. 2015;21(1):39–50.

62. Donnelly BF, et al. Hsp70 and Hsp90 multichaperone complexes sequentially regulate thiazide-sensitive cotransporter endoplasmic reticulum-associated degradation and biogenesis. *J Biol Chem*. 2013;288(18):13124–13135.

63. Alzamora R, et al. AMP-activated protein kinase inhibits KCNQ1 channels through regulation of the ubiquitin ligase Nedd4-2 in renal epithelial cells. *Am J Physiol Renal Physiol*. 2010;299(6):F1308–F1319.

64. Hallows KR, et al. AMP-activated protein kinase inhibits alkaline pH- and PKA-induced apical vacuolar H+-ATPase accumulation in epididymal clear cells. *Am J Physiol Cell Physiol*. 2009;296(4):C672–C681.

65. Thastrup JO, et al. SPAK/OSR1 regulate NKCC1 and WNK activity: analysis of WNK isoform interactions and activation by T-loop trans-autophosphorylation. *Biochem J*. 2012;441(1):325–337.

66. Xu BE, Min X, Stippec S, Lee BH, Goldsmith EJ, Cobb MH. Regulation of WNK1 by an autoinhibitory domain and autophosphorylation. *J Biol Chem*. 2002;277(50):48456–48462.

67. Bruce MC, Kanelis V, Fouladkou F, Debonneville A, Staub O, Rotin D. Regulation of Nedd4-2 self-ubiquitination and stability by a PY motif located within its HECT-domain. *Biochem J*. 2008;415(1):155–163.

68. Vallon V, Schroth J, Lang F, Kuhl D, Uchida S. Expression and phosphorylation of the Na+-Cl- cotransporter NCC in vivo is regulated by dietary salt, potassium, and SGK1. *Am J Physiol Renal Physiol*. 2009;297(3):F704–F712.